Hyperspectral longwave infrared reflectance spectra of dry anthropogenic plastics and natural materials

Shungudzemwoyo P. Garaba [1], Tomás Acuña-Ruz [2] and Cristian B. Mattar [3]

[1]Marine Sensor Systems Group, Institute for Chemistry and Biology of the Marine Environment, Carl von Ossietzky University of Oldenburg, Schleusenstraße 1, Wilhelmshaven 26382, Germany
[2] Laboratory for Analysis of the Biosphere (LAB), University of Chile, Av. Santa Rosa 11315, La Pintana Santiago. Chile.
[3] Laboratory of Geosciences (Geolab), University of Aysén, Obispo Vielmo 62, Coyhaique, Chile.

Correspondence to: Shungudzemwoyo P. Garaba (shungu.garaba@uni-oldenburg.de)

Abstract

Remote sensing of litter is foreseen to be an important source of additional information relevant to scientific awareness about plastic pollution. Here, we document directional hemispherical reflectance measurements of anthropogenic and natural materials gathered along the shorelines of Chiloé Archipelago, Chile. These spectral observations were completed in a laboratory using a state-of-the-art hyperspectral HyLogger-3™ spectrometer in the thermal infrared (TIR) region; medium wave infrared (6000 nm) to long wave infrared (14500 nm) spectrum at 25 nm intervals. The samples we investigated included sands, shells, algae, nautical ropes, Styrofoam®, gunny sacks and several fragments of plastic based items. The visible colours of these samples included shades of black, blue, brown, green, orange, white and yellow. We grouped the samples using robust statistical approaches (derivatives, peak seeking technique) and visual analyses of the derived hyperspectral reflectances. In each group we derived the average or TIR end-member signal as well as deduced diagnostic wavebands. Most of the diagnostic wavebands picked were found to be inside the atmospheric window of the TIR spectrum region. Furthermore, this laboratory reference dataset and findings might become useful in related field observations using similar thermal infrared technologies, especially in identifying anomalies resulting from environmental and meteorological perturbations. Validation and verification of proposed diagnostic wavebands would be part of a continuing effort to advance TIR remote sensing knowledge as well as assist robust detection algorithm development to potentially distinguish plastics in litter throughout the natural environments. Data is available in open-access via the online repository PANGAEA database of the World Data Centre for Marine Environmental Sciences https://doi.pangaea.de/10.1594/PANGAEA.919536 (Acuña-Ruz and Mattar B., 2020).

1 Introduction

Investigations focused on remote sensing technologies with 'detect, identify, quantify, track' capabilities for floating plastic litter in the blue planet are gaining momentum (Garaba and Dierssen, 2020;Maximenko et al., 2016). Consequently, there has been a rising number of exploratory research gathering spectral information in the ultraviolet (UV, 350 nm) to shortwave infrared (SWIR, 2500 nm) spectrum. In these studies, multi to hyperspectral reflectance signatures of plastic litter were

gathered in laboratories, over land as well as in aquatic environments from handheld, unmanned aerial systems, aircraft and satellite platforms (Garaba et al., 2018;Topouzelis et al., 2019;Acuña-Ruz et al., 2018;Goddijn-Murphy and Dufaur, 2018). Likewise, stakeholders in collaboration with remote sensing scientists have been dedicating resources to examine opportunities of leveraging descriptor information or proxy end-products from these technologies to support monitoring of plastic litter.

An interdisciplinary team of experts recently proposed some initial requirements and capabilities for future sensors relevant to the detection of plastics in terms of temporal and geo-spatial resolutions (Martínez-Vicente et al., 2019). Despite the need for new sensors alongside the current suite, remote sensing technologies ought to offer integrated, affordable and sustainable monitoring strategy (Maximenko et al., 2016;G20, 2017;Werner et al., 2016). Furthermore, there is a research gap in scientific

10   evidence-based assessments that have utilized a combined wide range of current in-situ, airborne and spaceborne remote sensing tools to monitor plastic litter in the blue and green planet. Technologies with potential applications include synthetic aperture radar, polarimeters, light detection and ranging, microwave, thermal infrared imaging (Goddijn-Murphy and Williamson, 2019;van Sebille et al., 2020;Garaba et al., 2018;Lebreton et al., 2018). Thermal infrared (TIR) sensors have been shown to be suitable and effective in collecting information about heterogeneous targets such as clouds, rare earth elements,

15   soils, oil (hydrocarbon) spills even tracking whales or ships at sea (Laakso et al., 2019;Salisbury et al., 1987;Cuyler et al., 1992;Sobrino et al., 2009;Becker et al., 1981;Salisbury et al., 1993;Kuenzer and Dech, 2013;Hulley and Hook, 2008). The scientific evidence-based knowledge gained already from prior works on TIR remote sensing of oil, a natural hydrocarbon, can be utilized to investigate prospects of detecting floating plastic litter because plastics found in floating aquatic litter has been identified to be mostly synthetic hydrocarbons (GESAMP, 2015;Thevenon et al., 2014).

20

The framework of this work is therefore to highlight hyperspectral reflectance measurements of anthropogenic and natural objects conducted in the medium wave (MWIR – 6000 nm) to long wave infrared (LWIR – 14000 nm) spectrum. We further characterize the observed spectral reflectance properties and identify distinguishing features using robust statistical techniques. Within the scope of our study, we did not further discriminate the sand, algae and polymer types within the samples as focus

25   was on overall identification of optical properties of plastics in marine or washed ashore litter. Our hyperspectral reference library established and explained in this study further improves scientific knowledge about TIR characteristics of natural and anthropogenic plastic material. We believe such knowledge is essential in remote sensing algorithm development and defining future mission requirements (signal to noise, diagnostic wavebands, bandwidth, spatial or spectral resolution).

2 Methods and Materials

30   ### 2.1 Samples

Litter was gathered along the shorelines of Punta Mallil-Cuem, Detif and Punta Apabón on Chiloé Archipelago, Los Lagos region of Chile, from January to February 2017. Synthetic and manmade litter items included buoys, nautical ropes, fish nets,

meshes, plastic bottles, bags, strapping bands, tubings, gunny sacks, Styrofoam®, ordinary ropes, placemats (**Figure 1**). Visual inspection of litter samples suggested short to long term exposure to natural weathering processes in the environment. Qualitative analyses of the litter were focussed on the apparent colour, shape and form, factors that were used to predict the original state of the individual objects. Observed apparent colours of litter included shades of black, blue, brown, green, orange,

5   white and yellow. Each of these items had a size of at least 0.5 m² thus falling in the category of macroplastics (diameter > 5 mm). Other samples gathered were natural materials like local sand, rocks, shells and algae or vegetation for comparison purposes. Were believe the samples collected represented a majority of anthropogenic plastic and natural materials found along the shorelines of Chiloé Archipelago and was consistent with samples from a multi-year survey of other regions in Chile (Thiel et al., 2013).
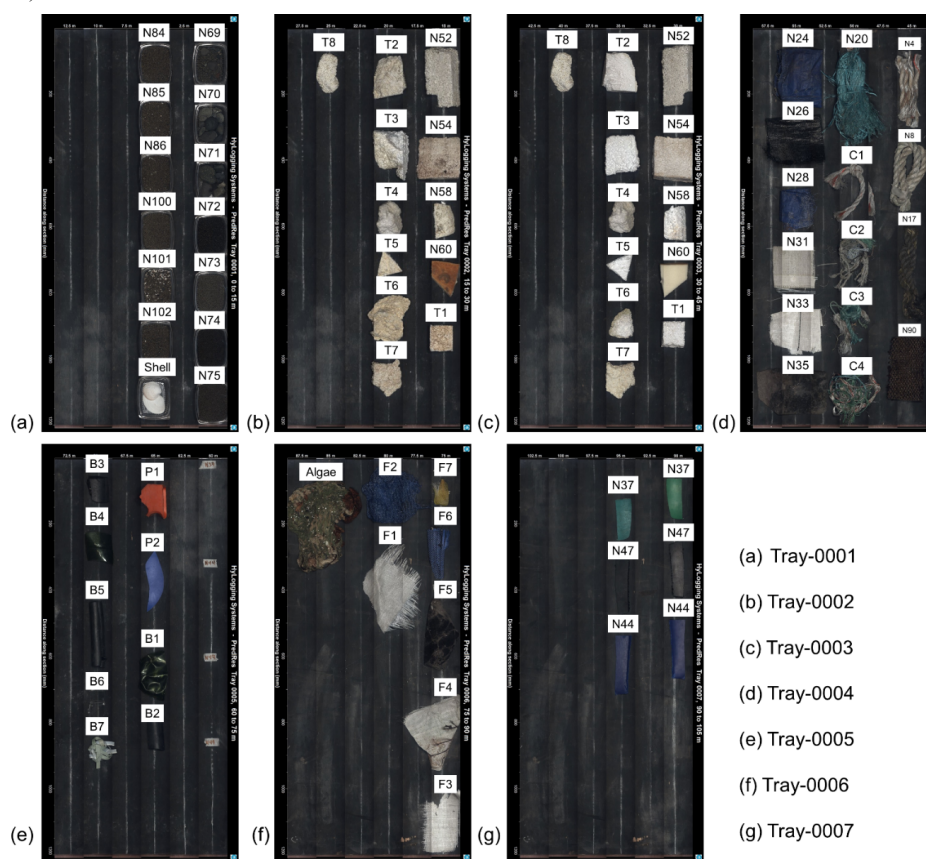
(a) Tray-0001

(b) Tray-0002

(c) Tray-0003

(d) Tray-0004

(e) Tray-0005

(f) Tray-0006

(g) Tray-0007

Figure 1. (a-g) Dry anthropogenic plastic and natural samples collected along the shorelines of Punta Mallil-Cuem, Detif and Punta Apabón on Chiloé Archipelago, Chile from January to February 2017 placed on black trays for hyperspectral hemispherical reflectance measurements using the HyLogger-3™ spectrometer.

2.2 Directional hemispherical reflectance measurements

Thermal infrared spectral measurements between 6000 and 14500 nm were obtained in 25 nm steps using the laboratory hyperspectral HyLogger-3™ spectrometer (Schodlok et al., 2016). A 10 x 10 cm Labsphere Infragold® diffuse plaque was used as a referencing standard to determine the hemispherical reflectance. Dry samples were placed on black tray that was labelled before scanning. The instrument was put in automatic mode to record along-track, a measurement was recorded as an average of continuous scans. Number of scans per object was therefore depended on the length, here ranging between 12 to 99 scans. The average object scan size was 16 mm. Detector window was at 0 ° nadir viewing angle with dual 800 °C blackbody radiation sources at 20 ° nadir angle. A true colour image was also captured during the scanning of each subset placed on the tray. All together 76 spectra were utilized for this study.

2.3 Data analyses

Processing of collected data was performed in MathWorks MATLAB R2016a. Descriptive statistics of spectral reflectances were determined for each respective object namely mean, standard deviation and median. Location of absorption features were the main descriptors of spectra, a common technique in remote sensing (Garaba and Dierssen, 2020;Dierssen and Garaba, 2020;Huguenin and Jones, 1986). Locations of absorption features were derived using a modified and robust scale-space peak algorithm (Liutkus, 2015). Instead of identifying the peaks in the measured spectra, we first inverted the spectra to transform the actual peaks into absorption features whilst making the absorption features into peaks. After peak waveband identification the measured spectra were smoothed using a moving average filter with a window of 3 nm, second derivatives were computed using 3-point central differences. No quantitative spectral shape evaluation was conducted because the analyses completed were considered appropriate to objectively classify and characterise the spectra available. An inter-comparison of the absorption features identified by the modified scale-space peak algorithm and the matching peaks in the second derivative signals we determined diagnostic absorption features and representative end-members of the materials investigated in this study. Unbiased percentage difference (UPD) was computed to determine the variability between observed spectra for each group of associated materials as proposed in prior studies (Garaba and Zielinski, 2013;Hooker et al., 2002;Garaba et al., 2015).

3 Results

3.1 Natural materials

3.1.1 Sands

A total of thirteen dark looking sand samples were gathered along the shorelines. The measured reflectances varied in terms

5   of magnitude over the measured wavebands (UPD: mean = 118 ± 26 % min = 67 %, max = 170%). Sample N72 and N74 had the lowest reflectances which can be attributed to their apparent colours as the darkest targets, hence less reflective (**Figure 1a**). These sands had a generally flat signal from 6000 to 7800 nm, except for samples N101 that consisted of a mix of sand and shiny fragments of shell (**Figure 1a**). We assume these fragments resulted in the peak observed between 6400 and 6800 nm. A TIR edge was noted at ~7800 nm in all the measurements of the sand samples. Highest reflectance values were identified

10 between 9000 and 10000 nm, except for sample N85 at ~8300 nm. There was a rapid decrease in reflectance from 10000 nm to 12700 nm followed by a gradual change up to 14500 nm (**Figure 2**).
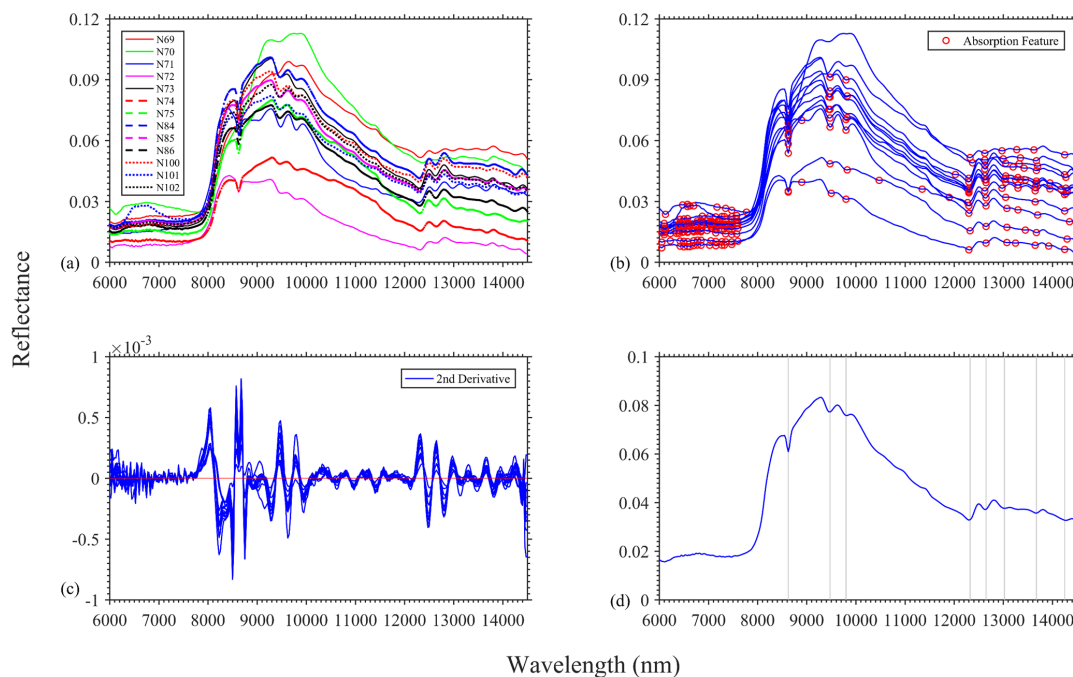
Figure 2. (a) Spectral reflectance of sands gathered along the shorelines of Punta Mallil-Cuem, Detif and Punta Apabón on Chiloé Archipelago, Chile, (b) absorption features automatically picked, (c) second derivatives spectra and (d) an end-member signal with the

15 proposed diagnostic absorption features highlighted by the vertical lines.

3.1.2 Shells

The apparent colour of typical shells found in the Los Lagos region of Chile were off white (**Figure 1a**). Over the measured spectrum the highest reflectance was observed at ~6800 nm, marked by the TIR edge around ~6100 nm. Major rapid increase and decrease in reflectance were located between 6000 and 7100 nm as well as 11000 and 11800 nm, suggesting two tailing

5   shaped peaks. Beyond the reflectance peak at ~6800 nm, there was a gradual decrease in the measured reflectance with an exception of the peak at 11625 nm (**Figure 3**).
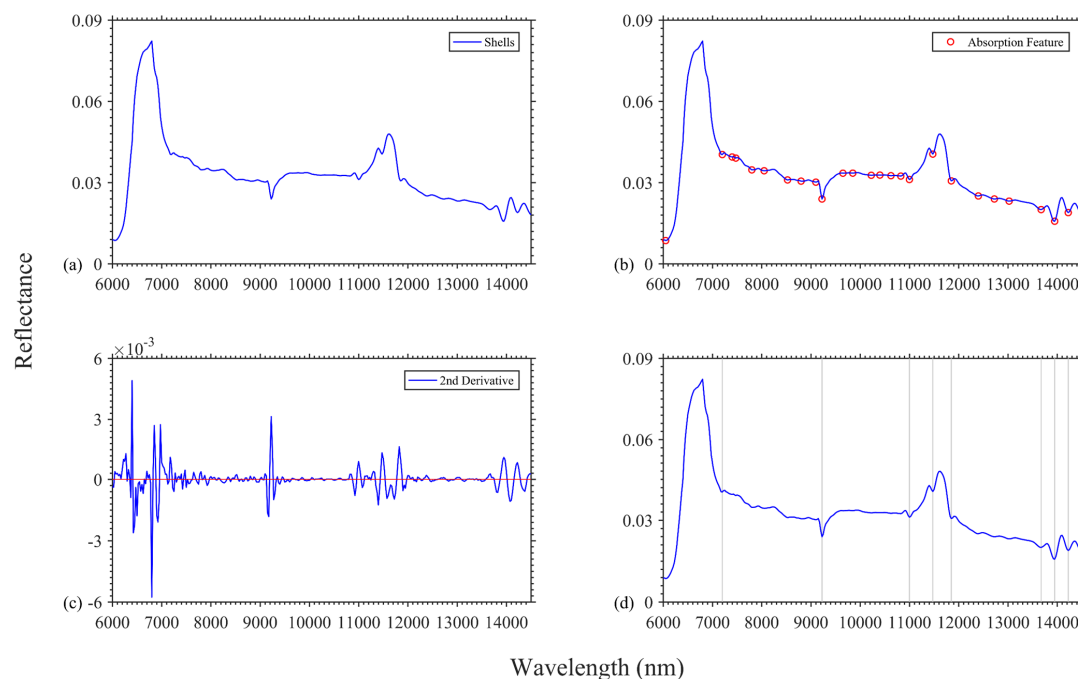
Figure 3. (a) Spectral reflectance of shells gathered along the shorelines of Punta Mallil-Cuem, Detif and Punta Apabón on Chiloé Archipelago, Chile, (b) absorption features automatically picked, (c) second derivatives spectra and (d) an end-member signal with the
10   proposed diagnostic absorption features highlighted by the vertical lines.

3.1.3 Algae

A dark green algae sampled was sampled and it had shiny pieces **(Figure 1f)**. Negative reflectances were observed in the wavebands above 12000 nm which suggested very strong absorption or detection limits of the sensor. Highest reflectance was at ~9450 nm which was followed by a rapid decrease until 9675 nm and then another major loss in reflectivity between 10600

15   and 1200 nm (**Figure 4**).
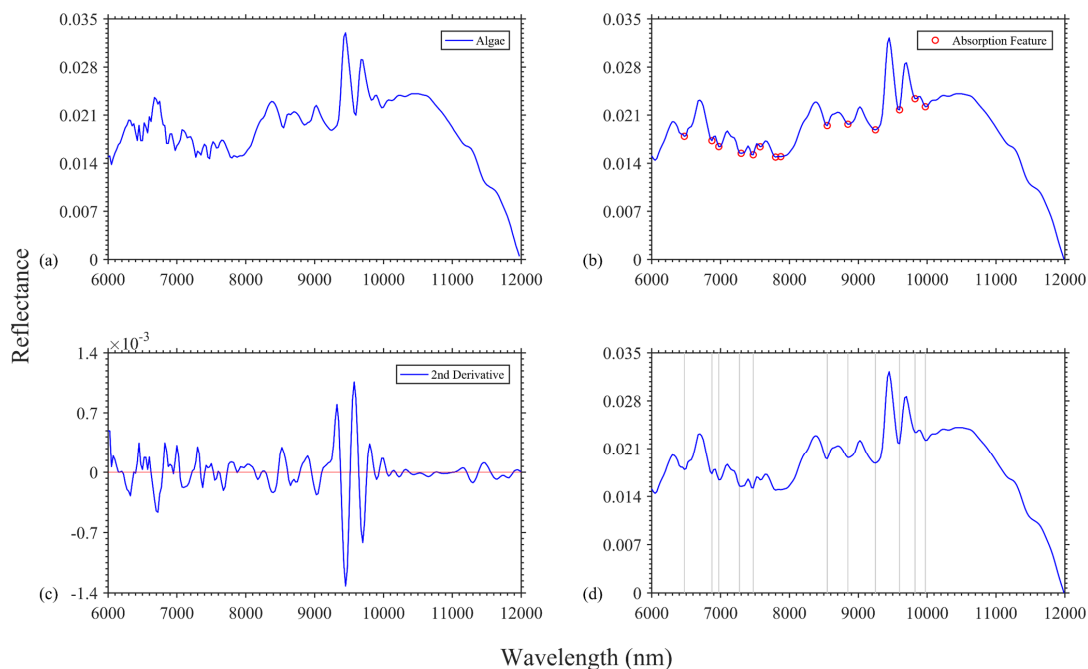
Figure 4. (a) (a) Spectral reflectance of algae found along the shorelines of Punta Mallil-Cuem, Detif and Punta Apabón on Chiloé Archipelago, Chile, (b) absorption features automatically picked, (c) second derivatives spectra and (d) an end-member signal with the proposed diagnostic absorption features highlighted by the vertical lines.

3.2 Anthropogenic materials

3.2.1 Styrofoam®

Spectral measurements were completed on 11 white coloured Sytrofoam® objects. Visual inspection of the top side of these pieces suggested exposure to dirt or various forms of chemical and physical weathering (**Figure 1**). The respective inside cut was relatively clean in comparison to the outside portion. The spectral shape was close to a sinusoidal curve with relatively

10   broad peaks, narrow troughs and characterized by a slow decreasing trend in the reflectance. At longer wavebands (>12000 nm) the troughs were wider and the peaks slightly narrower relative to the wavebands below 12000 nm. We noted the highest reflectances below 7000 nm and decreased gradually above 14000 nm. Sytrofoam® materials were the brightest targets investigated in this study and the reflectance magnitude differ over the measured wavebands (UPD: mean= 79 ± 16 %, min = 47 %, max = 120 %). Based on the determined reflectances the darkest target was upper side of N54 (**Figure 1b** and **Figure**

15   **5a**) and the brightest was bottom side of T3 (**Figure 1c** and **Figure 5a**).
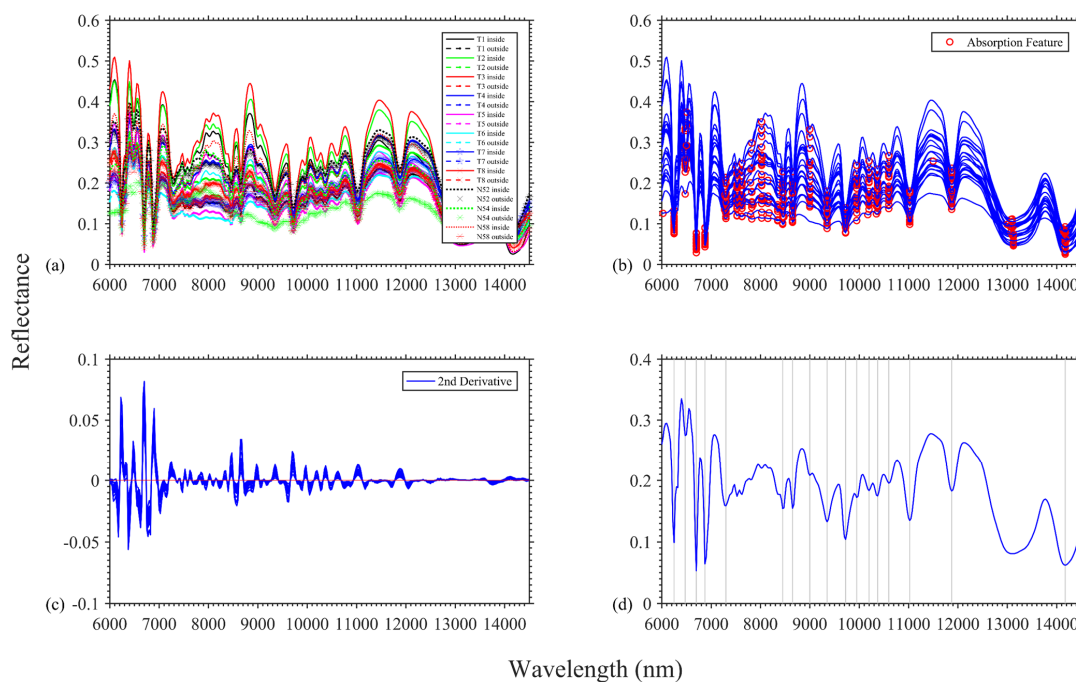
Figure 5. (a) Spectral reflectance of Sytrofoam® pieces found on the shorelines of Punta Mallil-Cuem, Detif and Punta Apabón on Chiloé Archipelago, Chile, (b) absorption features automatically picked, (c) second derivatives spectra and (d) an end-member signal with the proposed diagnostic absorption features highlighted by the vertical lines.

5   **3.2.2 Nautical ropes and straps**

Resemblances in the sinusoidal spectral shapes were salient in spectra from Sytrofoam® materials (**Figure 5**) and those of the nautical ropes as well as straps (**Figure 6**). The spectra had slightly broad peaks and narrow troughs (**Figure 6a**). We determined a generally steady increasing trend in the reflectance from the mid to the longwave infrared spectrum. Large differences in reflectance magnitude were in the longer wavebands above 13000 nm (UPD: mean = 70 ± 13 %, min = 48 %,

10   max = 101 %). On average the highest reflectances were located at ~13000 nm (**Figure 6d**). The darkest target in this group was the nautical rope N17 exhibiting lowest reflectances especially for wavebands below 6700 nm and above 10600 nm (**Figure 1d** and **Figure 6a**).
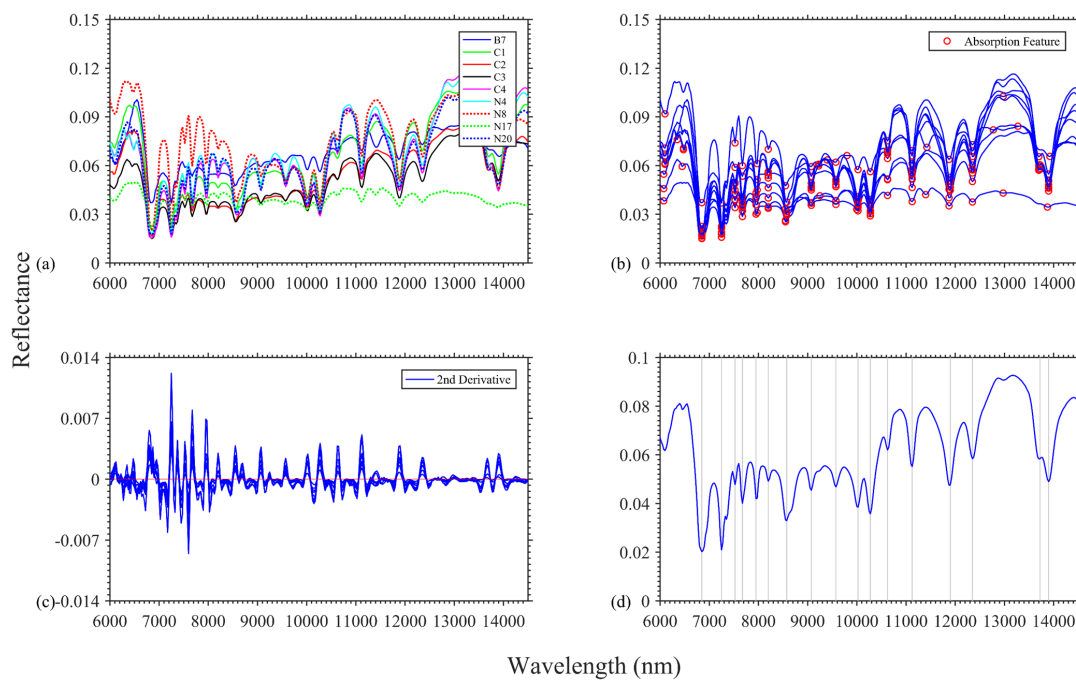
Figure 6. (a) Spectral reflectance of nautical ropes and straps found on the shorelines of Punta Mallil-Cuem, Detif and Punta Apabón in Chiloé Archipelago, Chile, (b) absorption features automatically picked, (c) second derivatives spectra and (d) an end-member signal with the proposed diagnostic absorption features highlighted by the vertical lines.

3.2.3 Gunny sacks

The apparent colours of the sacks were shades of white (F1, F3, F4, N31, N33), blue (F6) and black (N26). These whitish objects had higher reflectances compared to the darker objects within the sampled gunny sacks class (**Figure 1d**, **Figure 1f** and **Figure 7a**). Variations in the magnitude of spectra were determined to be highest below 6800 nm and longer wavebands above 14000 nm (UPD: mean = 88 ± 17 %, min = 58 %, max = 133 %). Compared the narrow troughs, the peaks were wider and there was a moderate increasing trend in reflectance from the mid to longwave infrared.
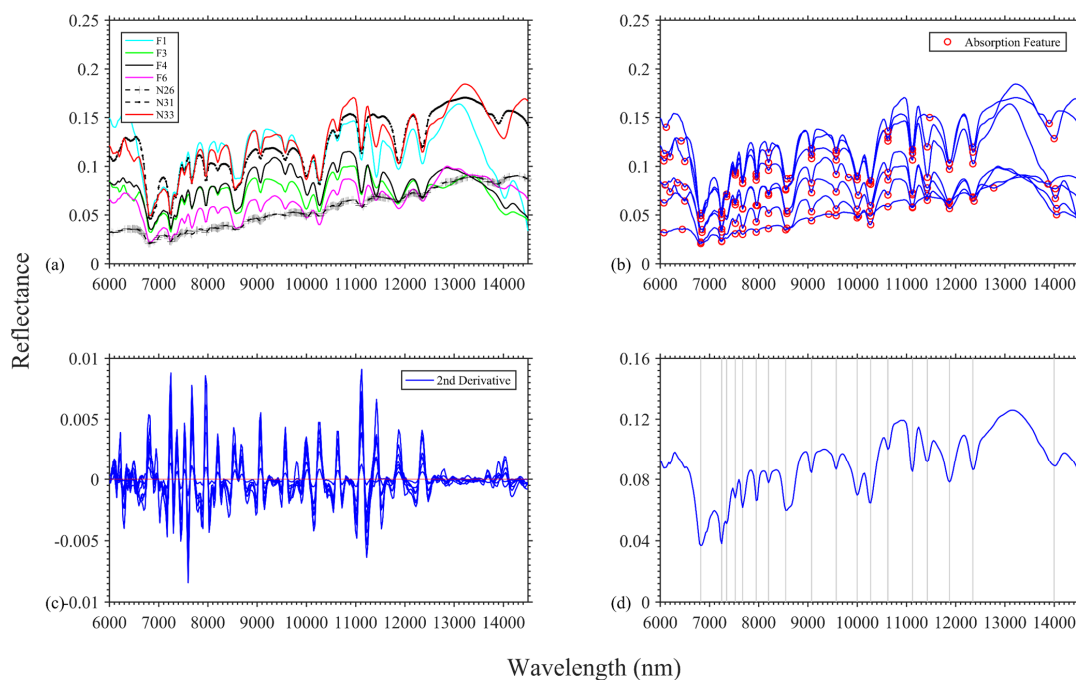
Figure 7. (a) Spectral reflectance of gunny sacks found along the shorelines of Punta Mallil-Cuem, Detif and Punta Apabón in Chiloé Archipelago, Chile, (b) absorption features automatically picked, (c) second derivatives spectra and (d) an end-member signal with the proposed diagnostic absorption features highlighted by the vertical lines.

5 **3.2.4 Fragments**

The apparent colours of collected plastic fragments varied in shades of orange (P1), blue (N44, P2), green (N37) and black (B2, B3, B5, N44). We presumed they had undergone natural weathering based on visual inspection indicated by the scratches and loss of colour (**Figure 1e** and **Figure 1g**). Interestingly, the darker targets N44 and B5 were revealed to be more reflective relative to the slightly brighter fragment the blue P2 (**Figure 1e** and **Figure 8a**). The measured reflectances of the fragments

10 exhibited considerable increasing trends from the mid to the longwave infrared spectrum (**Figure 8**). However, there were large margins between the less and most reflective samples (UPD: mean = 121 ± 5 %, min = 108 %, max = 129 %). On average the lowest reflectance was observed at ~6800 nm and the highest at 14000 nm that indicated a significant increasing trend (**Figure 8d**). V-shaped troughs were found at ~6800 nm followed by U-shaped troughs between 13500 and 14000 nm, a wide plateau was identified at ~9800 nm as well as peaks that had near rounded and tailing shapes.
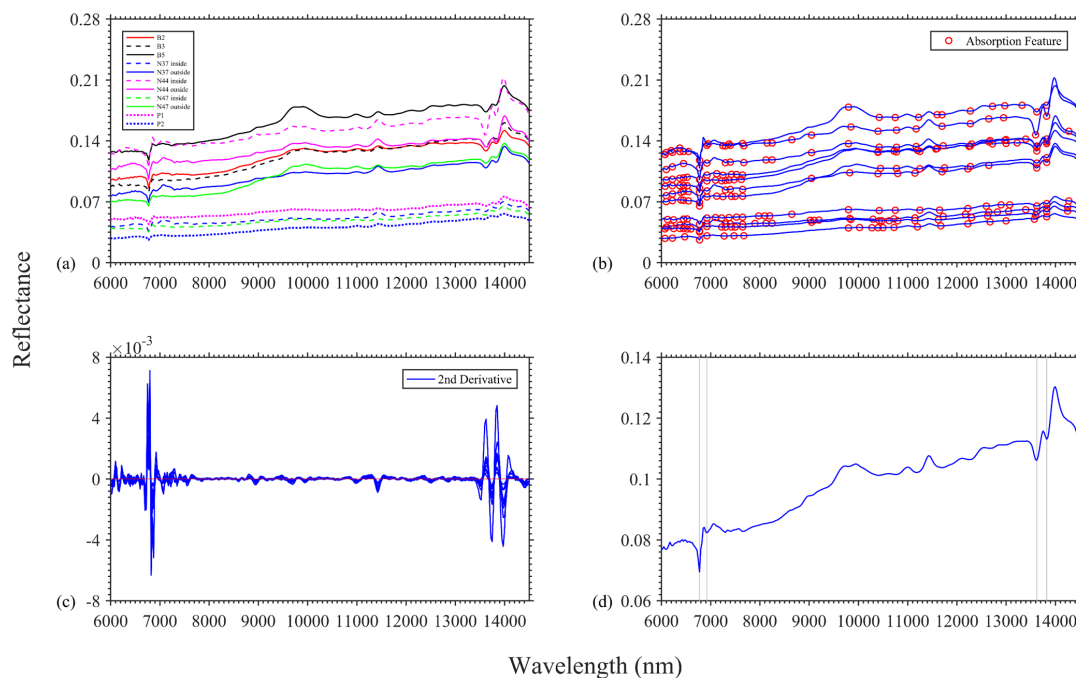
Figure 8. (a) Spectral reflectance of fragmented plastic objects found along the shorelines of Punta Mallil-Cuem, Detif and Punta Apabón on Chiloé Archipelago, Chile, (b) absorption features automatically picked, (c) second derivatives spectra and (d) an end-member signal with the proposed diagnostic absorption features highlighted by the vertical lines.

5 **3.2.5 Other plastics**

Objects B1, B4 and B6 has a similar spectral that had four major tailing peaks marked by a steady increasing trend from MWIR to LWIR (**Figure 9a**). The highest reflectance was found in the shiny green item B4 followed by the less shiny object B1 and the lowest was in the transparent strip B6 (**Figure 1e**) with large variations (UPD: mean = 89 ± 11 %, min = 59 %, max = 113 %). A blue (F2) and brownish (F7) piece were determined to have nearly rounded peaks (**Figure 1f**). Between 9000 and 13000

10 the range of reflectance was less than 20 % but increased rapidly from 13500 nm to reach 194 % (UPD: mean = 30 ± 39 %, min = 0 %, max = 194 %). Around 12000nm we observed the highest reflectance and in general there was a gradual increasing trend in the signal (**Figure 9b**). Black coloured materials F5 (**Figure 1f**) and N35 (**Figure 1d**) showed a significant rising trend in reflectance and generally well-rounded peaks with some tailing as well as fronting peaks (**Figure 9c**). The range was moderate for these black materials (UPD: mean = 39 ± 8 %, min =23 %, max = 61 %). Blue patches N24 and N28 (**Figure 1d**)

15 exhibited narrow to u-shaped troughs and sharp round or symmetric peaks (**Figure 9d**). There was a gradual increasing trend in the reflectance and it had a small range (UPD: mean = 4 ± 3 %, min = 0 %, max = 13 %). Two sides of a single white

presumed polyurethane foam piece N60 (**Figure 1b** and **Figure 1c**) had a strong increasing trend in reflectance from the MWIR to LWIR (**Figure 9e**). The bright whitish side was more reflective **(Figure 1c)** compared to the dark brownish portion (**Figure 1b**) variations were also small (UPD: mean = 13 ± 7 %, min =3 %, max = 44 %). These difference were higher in the MWIR and lowest towards the LWIR characterised by tailing, rounded and fronting peaks as well some narrow troughs (**Figure 9e**).

5   A dark pieces of a cargo strap N90 (**Figure 1d**) was not very reflective compared to all the materials observed in this study from the MWIR to LWIR spectrum (**Figure 9f**). The measured reflectance peaked around 11600 nm and the signal had a gradual increasing trend. Most of the peaks were rounded with some minor fronting and tailing shapes.
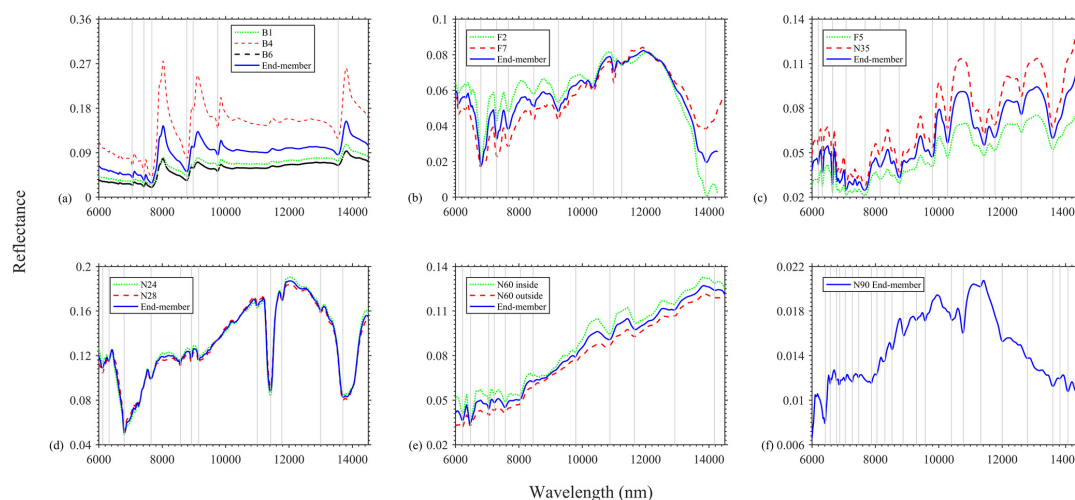
10   **Figure 9.** (a-f) Spectral reflectance of other anthropogenic materials in **Figure 1** gathered along the shorelines of Punta Mallil-Cuem, Detif and Punta Apabón on Chiloé Archipelago, Chile. An end-member spectrum is proposed with diagnostic absorption features highlighted by the vertical lines.

3.3 Diagnostic absorption features

We identified diagnostic absorption features of the measured materials based on a combination of visual inspection, modified
15   robust scale-space peak algorithm and second derivative analyses (**Table 1**).

4 Discussion

The samples we investigated were presumed to be a reasonable or appropriate subset of material commonly found along the shorelines of Chiloé Archipelago, Chile. Specifically Styrofoam®, gunny sacks and nautical ropes or the broken down fragments are typical waste products of blue economic activities including the vast aquaculture farming in the waters of Chiloé
20   (FAO, 2005;Thiel et al., 2013;Pozo et al., 2019;Gómez et al., 2020). However, it is important to note that our subset does not

necessarily represent each and every anthropogenic and natural litter item found on Chiloé Archipelago. Global reports have already shown that there is a huge diversity in polymers, colours, sizes and shapes of plastic found in marine litter (GESAMP, 2015;Lebreton et al., 2018;Thevenon et al., 2014;Thiel et al., 2013). We therefore believe our sample subset provides invaluable complementary insights to the interdisciplinary scientific evidence-based knowledge of global plastic litter.

Table 1. Location of proposed diagnostic absorption features derived from spectral measurements of samples from the shorelines of Punta Mallil-Cuem, Detif and Punta Apabón on Chiloé Archipelago, Chile.

Material	Location of Absorption Features (nm)
Sands	8625, 9475, 9800, 12325, 12650, 13025, 13675, 14250
Shells	7200, 9225, 11000, 11475, 11850, 13675, 13950, 14225
Algae	6475, 6875, 6975, 7275, 7475, 8550, 8850, 9250, 9600, 9825, 9975
Styrofoam®	6250, 6475, 6700, 6875, 7300, 8450, 8650, 9000, 9350, 9725, 9950, 10200, 10375, 10600, 11025, 11875, 14175
Nautical Ropes and Straps	6850, 7250, 7525, 7675, 7950, 8200, 8575, 9075, 9575, 10025, 10275, 10625, 11125, 11900, 12350, 13725, 13900
Gunny Sacks	6825, 7250, 7350, 7525, 7675, 7950, 8200, 8550, 9075, 9575, 10000, 10275, 10625, 11125, 11425, 11875, 12350, 14000
Fragments	6775, 6925, 13625, 13825
Other Plastics	- 7050, 7425, 7675, 8775, 8975, 9750, 13550; - 6100, 6325, 6800, 7300, 7675, 8475, 9250, 10350, 11000, 11250, 13900; - 6200, 6325, 6650, 7075, 7675, 8150, 8750, 9800, 10275, 11425 11775, 12600, 13600; - 6125, 6325, 6800, 7650, 8575, 8925, 9150, 11000, 11425, 11775, 13000, 13700; - 6225, 6475, 7050, 7225, 7575, 8050, 8450, 9800, 10875, 11650, 12925, 14175; - 6425, 6575, 6775, 6875, 7050, 7275, 7475, 7875, 8050, 8300, 8525, 8875, 9300, 9575, 10400, 10775, 11325 12000 12800, 13600, 13825, 14075, 14425;

We also identified several diagnostic absorption features (**Table 1**). Here, we conclude that an inter-comparison with prior

10   studies was challenging, primarily because we present some of the only few open-access hyperspectral reflectance observations in the MWIR to LWIR spectrum. Here we did not conduct further analysis to include the soil types, algae types and source polymers descriptor. However, attaching such additional key descriptors would add value to our spectral measurements, thus likely to improve the end-products that can be derived from remote sensing tools. Furthermore, we are aware that remote sensing activities in the TIR might report observations in terms of emissivity instead of reflectance (Sobrino et al., 2009;Cuyler

15   et al., 1992). It does not present any practical limitations in terms of usage of our datasets because emissivity can be derived from hemispherical reflectance measurements by applying Kirchhoff's Law (Nicodemus, 1965;Salisbury et al., 1987).

In this work, measurements were completed in a controlled laboratory setup and therefore did not take into account the effects of environmental and meteorological perturbations that play a role in the TIR spectrum especially in natural conditions. To

20   this end, aquatic or land based feasibility research is required to decipher and identify scientific evidence-based capabilities of TIR remote sensing as a monitoring strategy for plastics in land or marine litter. We also noted that most of the proposed

diagnostic absorption features of the derived end-member spectra fall in the TIR atmospheric window ~7400 to ~14200 nm (**Table 1** and **Figure 10**). If the laboratory TIR measurements presented here were to be assumed to be Bottom-of-Atmosphere reflectances, we would expect to detect the diagnostic wavebands found in this study through an intervening atmosphere suggesting spectrally similar Top-of-Atmosphere reflectances. Validation and verification of this assumption would of course

5   involve radiative transfer simulations and in-situ spectral reference libraries. Satellite missions of interest include the ASTER from the National Aeronautics and Space Administration/Japansese Ministry of Economy Trade and Industry and Landsat-8 from the United States Geologic Survey as well as. ASTER and Landsat-8 ought to be evaluated for potential applications of detecting aggregated litter taking advantage of the spatial resolution ~ 100 m and TIR wavebands (**Figure 10**). We need to further emphasize that the atmospheric window in the TIR is relatively wide containing a sizeable number of diagnostic

10   wavebands of materials studied here were revealed in this spectrum region that could be observed by already available TIR satellites. The TIR atmospheric window seems to offer more opportunities to remotely sense anthropogenic plastics through an intervening atmosphere in comparison to those reported from studies covering ultraviolet to shortwave infrared spectral regions (Garaba and Dierssen, 2018).
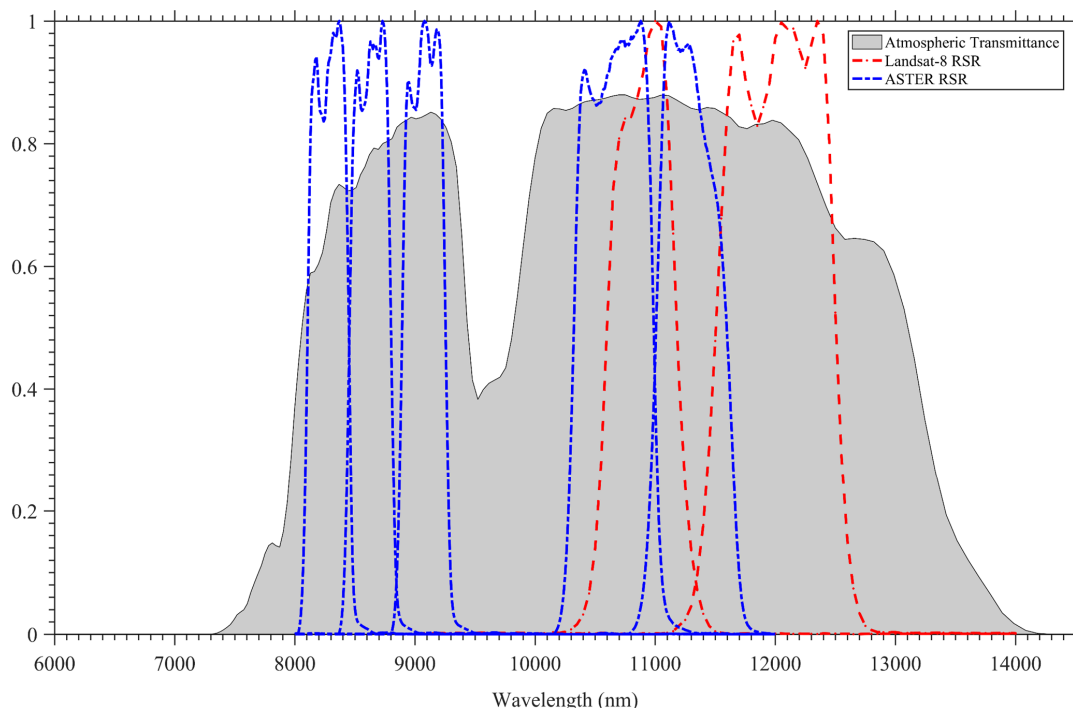
15   **Figure 10.** Atmospheric transmittance simulated using 1976 US Standard conditions at 0° zenith in LOWTRAN and the relative spectral response (RSR) function data of ASTER as well as Landsat-8 satellite missions.

4 Data availability

Quality control was performed according to the guidelines of SeaDataNet. Data is available in open-access via the online repository PANGAEA database of the World Data Centre for Marine Environmental Sciences https://doi.pangaea.de/10.1594/PANGAEA.919536 (Acuña-Ruz and Mattar B., 2020).

5 **5 Conclusions and outlook**

We report laboratory measurements of hyperspectral TIR hemispherical reflectances collected from natural and anthropogenic material. Remote sensing relevant to plastic litter in the TIR spectrum is gradually gaining research interest but not as fast as the studies based on the ultraviolet to shortwave infrared wavebands. A major drawback has been technological advances are mostly driven by societal and scientific needs to understand the blue and green planet. Here we exhibit a spectral reference

10 library that could be leveraged to exploit and investigate the feasibility of airborne, high altitude pseudo satellite or space hyperspectral TIR sensors as additional remote monitoring strategies of plastic litter because of the wide atmospheric window, meaning Top-of-Atmosphere derived variables will not require atmospheric correction. Use of datasets that do not require atmospheric correction mitigates the uncertainties related to the various assumption implemented in different algorithms to remove contributions by atmospheric gases among other optically active components detected by remote sensing tools.

15 Substantial work is thus required to further explore the prospects of TIR technologies as additional monitoring strategies to assist plastic litter research. Knowledge gained from studies involving plastic litter will benefit interdisciplinary science as more essential (biogeochemical and physical) proxy descriptors might be derived from current and future TIR satellite missions by agencies like European Space Agency, German Aerospace Centre, National Aeronautics and Space Administration and United States Geologic Survey.

20 **Author contribution**

SPG analysed the data and prepared the first draft of the manuscript. TAR and CBM designed and conducted the experiment. All authors discussed and approved the manuscript text.

Competing interests

The authors declare that they have no conflict of interest.

25 **Financial support**

The study was funded by Deutsche Forschungsgemeinschaft (grant no. 417276871), "Estudio para la generación de un modelo predictivo de residuos en 3 playas de Chiloé, mediante Teledetección Cuantitativa (PRED-RES Chiloé)", Agencia de Sustentabilidad y Cambio Climático (ASCC)/Sustainability Agency and Climate Change and the INNOVA CSIRO−CHILE 10CEII−9007 project (run by the HL3).

References

Acuña-Ruz, T., Uribe, D., Taylor, R., Amézquita, L., Guzmán, M. C., Merrill, J., Martínez, P., Voisin, L., and Mattar B, C.: Anthropogenic marine debris over beaches: Spectral characterization for remote sensing applications, Remote Sens. Environ., 217, 309-322, doi:10.1016/j.rse.2018.08.008, 2018.

Acuña-Ruz, T., and Mattar B., C.: Thermal infrared spectral database of marine litter debris in Archipelago of Chiloé, Chile, PANGAEA, doi:10.1594/PANGAEA.919536, 2020.

Becker, F., Ngai, W., and Stoll, M. P.: An active method for measuring thermal infrared effective emissivities: Implications
10 and perspectives for remote sensing, Adv. Space Res., 1, 193-210, doi:10.1016/0273-1177(81)90394-X, 1981.

Cuyler, L. C., Wiulsrød, R., and ØRitsland, N. A.: Thermal infrared radiation from free living whales, Mar. Mammal Sci., 8, 120-134, doi:10.1111/j.1748-7692.1992.tb00371.x, 1992.

15 Dierssen, H. M., and Garaba, S. P.: Bright Oceans: Spectral Differentiation of Whitecaps, Sea Ice, Plastics, and Other Flotsam, in: Recent Advances in the Study of Oceanic Whitecaps: Twixt Wind and Waves, edited by: Vlahos, P., and Monahan, E. C., Springer International Publishing, Cham, 197-208, 2020.

FAO: National Aquaculture Sector Overview. Visión General del Sector Acuícola Nacional - Chile., Food and Agriculture
20 Organization of the United Nations, Rome, Italy, 12, 2005.

G20: Annex to G20 Leaders Declaration: G20 Action Plan on Marine Litter, G20 Summit 2017, Hamburg, Germany (7-8 July), 2017.

25 Garaba, S. P., and Zielinski, O.: Comparison of remote sensing reflectance from above-water and in-water measurements west of Greenland, Labrador Sea, Denmark Strait, and west of Iceland, Opt. Express, 21, 15938-15950, doi:10.1364/OE.21.015938, 2013.

Garaba, S. P., Voß, D., Wollschläger, J., and Zielinski, O.: Modern approaches to shipborne ocean color remote sensing, Appl.
30 Opt., 54, 3602-3612, doi:10.1364/AO.54.003602, 2015.

Garaba, S. P., Aitken, J., Slat, B., Dierssen, H. M., Lebreton, L., Zielinski, O., and Reisser, J.: Sensing ocean plastics with an airborne hyperspectral shortwave infrared imager, Environ. Sci. Technol., 52, 11699-11707, doi:10.1021/acs.est.8b02855, 2018.

35

Garaba, S. P., and Dierssen, H. M.: An airborne remote sensing case study of synthetic hydrocarbon detection using short wave infrared absorption features identified from marine-harvested macro- and microplastics, Remote Sens. Environ., 205, 224-235, doi:10.1016/j.rse.2017.11.023, 2018.

40 Garaba, S. P., and Dierssen, H. M.: Hyperspectral ultraviolet to shortwave infrared characteristics of marine-harvested, washed-ashore and virgin plastics, Earth Syst. Sci. Data, 12, 77-86, doi:10.5194/essd-12-77-2020, 2020.

GESAMP: Sources, fate and effects of microplastics in the marine environment: a global assessment. (IMO/FAO/UNESCO-IOC/UNIDO/WMO/IAEA/UN/UNEP/UNDP Joint Group of Experts on the Scientific Aspects of Marine Environmental
45 Protection). GESAMP Report and Studies No. 90, International Maritime Organization - London, UK, 96, 2015.

Goddijn-Murphy, L., and Dufaur, J.: Proof of concept for a model of light reflectance of plastics floating on natural waters, Mar. Pollut. Bull., 135, 1145-1157, doi:10.1016/j.marpolbul.2018.08.044, 2018.

Goddijn-Murphy, L., and Williamson, B.: On thermal infrared remote sensing of plastic pollution in natural waters, Remote Sens. (Basel), 11, 2159, doi:10.3390/rs11182159, 2019.

5   Gómez, V., Pozo, K., Nuñez, D., Přibylová, P., Audy, O., Baini, M., Fossi, M. C., and Klánová, J.: Marine plastic debris in Central Chile: Characterization and abundance of macroplastics and burden of persistent organic pollutants (POPs), Mar. Pollut. Bull., 152, 110881, doi:10.1016/j.marpolbul.2019.110881, 2020.

Hooker, S. B., Lazin, G., Zibordi, G., and McLean, S.: An evaluation of above- and in-water methods for determining water-leaving radiances, J. Atmos. Ocean. Technol., 19, 486-515, doi: 10.1175/1520-0426(2002)019<0486:AEOAAI>2.0.CO;2
10 2002.

Huguenin, R. L., and Jones, J. L.: Intelligent information extraction from reflectance spectra: Absorption band positions, J. Geophys. Res. Solid Earth, 91, 9585-9598, doi:10.1029/JB091iB09p09585, 1986.

15 Hulley, G. C., and Hook, S. J.: A new methodology for cloud detection and classification with ASTER data, Geophys. Res. Lett., 35, doi:10.1029/2008gl034644, 2008.

Kuenzer, C., and Dech, S.: Thermal infrared remote sensing. In: Remote sensing and digital image processing, van der Meer, F. D., and Jarocińska, A. (Eds.), 17, Springer Netherlands, 2013.
20

Laakso, K., Turner, D. J., Rivard, B., and Sánchez-Azofeifa, A.: The long-wave infrared (8-12 μm) spectral features of selected rare earth element—Bearing carbonate, phosphate and silicate minerals, Int. J. Appl. Earth Obs. Geoinformation, 76, 77-83, doi:10.1016/j.jag.2018.11.005, 2019.

25 Lebreton, L., Slat, B., Ferrari, F., Sainte-Rose, B., Aitken, J., Marthouse, R., Hajbane, S., Cunsolo, S., Schwarz, A., Levivier, A., Noble, K., Debeljak, P., Maral, H., Schoeneich-Argent, R., Brambini, R., and Reisser, J.: Evidence that the Great Pacific Garbage Patch is rapidly accumulating plastic, Sci. Rep., 8, 4666, doi:10.1038/s41598-018-22939-w, 2018.

Liutkus, A.: Scale-space peak picking: Inria, Speech Processing Team, Available online on https://hal.inria.fr/hal-01103123,
30 Inria Nancy - Grand Est, Villers-lès-Nancy, France, 2015.

Martínez-Vicente, V., Clark, J. R., Corradi, P., Aliani, S., Arias, M., Bochow, M., Bonnery, G., Cole, M., Cózar, A., Donnelly, R., Echevarría, F., Galgani, F., Garaba, S. P., Goddijn-Murphy, L., Lebreton, L., Leslie, H. A., Lindeque, P. K., Maximenko, N., Martin-Lauzer, F.-R., Moller, D., Murphy, P., Palombi, L., Raimondi, V., Reisser, J., Romero, L., Simis, S. G. H., Sterckx,
35 S., Thompson, R. C., Topouzelis, K. N., van Sebille, E., Veiga, J. M., and Vethaak, A. D.: Measuring marine plastic debris from space: Initial assessment of observation requirements, Remote Sens. (Basel), 11, 2443, doi:10.3390/rs11202443, 2019.

Maximenko, N., Arvesen, J., Asner, G., Carlton, J., Castrence, M., Centurioni, L., Chao, Y., Chapman, J., Chirayath, V., Corradi, P., Crowley, M., Dierssen, H. M., Dohan, K., Eriksen, M., Galgani, F., Garaba, S. P., Goni, G., Griffin, D., Hafner,
40 J., Hardesty, D., Isobe, A., Jacobs, S., Kamachi, M., Kataoka, T., Kubota, M., Law, K. L., Lebreton, L., Leslie, H. A., Lumpkin, R., Mace, T. H., Mallos, N., McGillivary, P. A., Moller, D., Morrow, R., Moy, K. V., Murray, C. C., Potemra, J., Richardson, P., Robberson, B., Thompson, R., van Sebille, E., and Woodring, D.: Remote sensing of marine debris to study dynamics, balances and trends, Community White Paper Produced at the Workshop on Mission Concepts for Marine Debris Sensing, 22, 2016.
45

Nicodemus, F. E.: Directional Reflectance and Emissivity of an Opaque Surface, Appl. Opt., 4, 767-775, doi:10.1364/AO.4.000767, 1965.

Pozo, K., Gomez, V., Torres, M., Vera, L., Nuñez, D., Oyarzún, P., Mendoza, G., Clarke, B., Fossi, M. C., Baini, M., Přibylová, P., and Klánová, J.: Presence and characterization of microplastics in fish of commercial importance from the Biobío region in central Chile, Mar. Pollut. Bull., 140, 315-319, doi:10.1016/j.marpolbul.2019.01.025, 2019.

5   Salisbury, J. W., Walter, L. S., and Vergo, N.: Mid-infrared (2.1-25 um) spectra of minerals; first edition, U. S. Geological Survey, Report 87-263, 1987.

Salisbury, J. W., D'Aria, D. M., and Sabins, F. F.: Thermal infrared remote sensing of crude oil slicks, Remote Sens. Environ., 45, 225-231, doi:10.1016/0034-4257(93)90044-X, 1993.

Schodlok, M. C., Whitbourn, L., Huntington, J., Mason, P., Green, A., Berman, M., Coward, D., Connor, P., Wright, W., Jolivet, M., and Martinez, R.: HyLogger-3, a visible to shortwave and thermal infrared reflectance spectrometer system for drill core logging: functional description, Aust. J. Earth Sci., 63, 929-940, doi:10.1080/08120099.2016.1231133, 2016.

15   Sobrino, J. A., Mattar, C., Pardo, P., Jiménez-Muñoz, J. C., Hook, S. J., Baldridge, A., and Ibañez, R.: Soil emissivity and reflectance spectra measurements, Appl. Opt., 48, 3664-3670, doi:10.1364/AO.48.003664, 2009.

Thevenon, F., Carroll, C., Sousa, J., and (editors): Plastic debris in the ocean: The characterization of marine plastics and their environmental impacts, situation analysis report, International Union for Conservation of Nature, Gland, Switzerland, 52,
20   2014.

Thiel, M., Hinojosa, I. A., Miranda, L., Pantoja, J. F., Rivadeneira, M. M., and Vásquez, N.: Anthropogenic marine debris in the coastal environment: A multi-year comparison between coastal waters and local shores, Mar. Pollut. Bull., 71, 307-316, doi:10.1016/j.marpolbul.2013.01.005, 2013.

25

Topouzelis, K., Papakonstantinou, A., and Garaba, S. P.: Detection of floating plastics from satellite and unmanned aerial systems (Plastic Litter Project 2018), Int. J. Appl. Earth Obs. Geoinformation, 79, 175-183, doi:10.1016/j.jag.2019.03.011, 2019.

30   van Sebille, E., Aliani, S., Law, K. L., Maximenko, N., Alsina, J. M., Bagaev, A., Bergmann, M., Chapron, B., Chubarenko, I., Cózar, A., Delandmeter, P., Egger, M., Fox-Kemper, B., Garaba, S. P., Goddijn-Murphy, L., Hardesty, B. D., Hoffman, M. J., Isobe, A., Jongedijk, C. E., Kaandorp, M. L. A., Khatmullina, L., Koelmans, A. A., Kukulka, T., Laufkötter, C., Lebreton, L., Lobelle, D., Maes, C., Martinez-Vicente, V., Morales Maqueda, M. A., Poulain-Zarcos, M., Rodríguez, E., Ryan, P. G., Shanks, A. L., Shim, W. J., Suaria, G., Thiel, M., van den Bremer, T. S., and Wichmann, D.: The physical oceanography of
35   the transport of floating marine debris, 15, 023003, doi:10.1088/1748-9326/ab6d7d, 2020.

Werner, S., Budziak, A., van Franeker, J., Galgani, F., Hanke, G., Maes, T., Matiddi, M., Nilsson, P., Oosterbaan, L., Priestland, E., Thompson, R., Veiga, J., and Vlachogianni, T.: Harm caused by marine litter, Luxembourg: Publications Office of the European Union, 92, 2016.

40